Quantitation of liquid-crystalline ordering in F-actin solutions

Chris M. Coppin and Paul C. Leavis
Department of Physiology, Tufts University School of Medicine; and Department of Muscle Research, Boston Biomedical Research Institute, Boston, Massachusetts 02114 USA

ABSTRACT Actin filaments (F-actin) are important determinants of cellular shape and motility. These functions depend on the collective organization of numerous filaments with respect to both position and orientation in the cytoplasm. Much of the orientational organization arises spontaneously through liquid crystal formation in concentrated F-actin solutions. In studying this phenomenon, we found that solutions of purified F-actin undergo a continuous phase transition, from the isotropic state to a liquid crystalline state, when either the mean filament length or the actin concentration is increased above its respective threshold value. The phase diagram representing the threshold filament lengths and concentrations at which the phase transition occurs is consistent with that predicted by Flory's theory on solutions of noninteracting, rigid cylinders (Flory, 1956*b*). However, in contrast to other predictions based on this model, we found no evidence for the coexistence of isotropic and anisotropic phases. Furthermore, the phase transition proved to be temperature dependent, which suggests the existence of orientation-dependent interfilament interactions or of a temperature-dependent filament flexibility.

We developed a simple method for growing undistorted fluorescent acrylodan-labeled F-actin liquid crystals; and we derived a simple theoretical treatment by which polarization-of-fluorescence measurements could be used to quantitate, for the first time, the degree of spontaneous filament ordering (nematic order parameter) in these F-actin liquid crystals. This order parameter was found to increase monotonically with both filament length and concentration.

Actin liquid crystals can readily become distorted by a process known as "texturing." Zigzaging and helicoidal liquid crystalline textures which persisted in the absence of ATP were observed through the polarizing microscope. Possible texturing mechanisms are discussed.

INTRODUCTION

Actin is a ubiquitous cytoskeletal protein that plays an important role in the control of cell shape and certain modes of motility. Under physiological conditions, actin molecules (G-actin) self-assemble to form long, thin, moderately-flexible filaments (F-actin) that tend to spontaneously align with one another in order to fit within the available space (like sardines) (Kerst et al., 1990; Newman et al., 1988; Suzuki et al., 1991). An understanding of the cellular control of actin filament ordering is essential for the understanding of cytoskeletal organization as a whole. Highly ordered actin-rich domains can be found in the periphery of the cytoplasm in many cell types. Well known examples include the static brush border microvilli of intestinal epithelial cells (Bretsher, 1983; Mooseker, 1983; Mooseker and Howe, 1982), the static stereocilia of auditory epithelial hair cells (Tilney and Tilney, 1984), and dynamic protrusions at the surface of locomoting cells (Luduena and Wessells, 1973). The degree of filament ordering in the cytoplasm seems to be modulated by a variety of domain-specific actin binding proteins (Drenckhahn et al., 1991).

The spontaneous long range orientational ordering of randomly positioned filaments in solution is characteristic of a nematic liquid crystal. In a nematic, the filaments are oriented preferentially about an imaginary axis, called the "director," which defines the optic axis of the linearly birefringent solution.

To a first approximation actin filaments can be modeled as noninteracting, impenetrable, rigid cylinders in solution. Theoretical treatments of such a model (Flory, 1956*b*; Ishihara, 1951; Onsager, 1949) predict the entropy-dependent emergence of a nematic liquid crystalline phase when the cylinder concentration is raised past a first threshold that varies approximately inversely with cylinder length. As the concentration is further increased past a second threshold, which also varies inversely with cylinder length, the isotropic phase should vanish, leaving only a uniformly anisotropic phase. Between these two thresholds, an isotropic phase should coexist at equilibrium with a slightly more concentrated, anisotropic, liquid crystalline phase. The theory successfully accounts for the phase behavior of suspensions of tobacco mosaic virus, a particle that conforms well to the rigid cylinder model (Oster, 1950). Statistical thermodynamic treatment of a more general model predicts that the difference in concentration between the isotropic and anisotropic phases, known as the miscibility gap, will increase with increasing cylinder flexibility, polydispersity in length, and intercylinder interactions (Flory, 1956*a*; Flory, 1978; Flory, 1984; Flory and Frost, 1978; Flory and Ronca, 1979). This means that experimentally one would expect a phase separation of F-actin solutions under a wide range of conditions.

Previous investigations with F-actin solutions have demonstrated the spontaneous emergence of long range

Address correspondence to Dr. P. Leavis, Department of Muscle Research, Boston Biomedical Research Institute, 20 Staniford Street, Boston, MA 02114.

0006-3495/92/09/794/14 $2.00

orientational ordering of the filaments (Kerst et al., 1990; Newman et al., 1988; Suzuki et al., 1991). Whether the published observations (Newman et al., 1988; Suzuki et al., 1991) revealed a coexistence of isotropic and anisotropic phases at equilibrium, however, is subject to interpretation.

Investigating the effects of various physiological factors, such as actin binding proteins, actin concentration, filament length, etc., on the filaments' orientational organization, demands a nonperturbating measurement of the quantitative degree of filament organization expressed on an absolute scale. To our knowledge, previous studies have been confined to measurements of the linear birefringence of F-actin solutions (Suzuki et al., 1991). Whereas the latter approach can prove useful for comparing, in a semiquantitative way, the relative degree of ordering in different samples, it cannot provide the absolute degree of ordering defined in terms of an orientational distribution (because the anisotropy of the polarizability of the actin filament is unknown). To determine the absolute degree of ordering another approach was needed.

Polarized fluorescence has been shown in the past to be a valuable method for investigating orientational ordering of macromolecules in biological systems (see for example Burghardt, 1984; Burghardt, 1985; Burghardt and Ajtai, 1988). In particular, this approach has been used successfully in the study of myosin-head orientation in muscle fibers (see for example Mendelson and Wilson, 1987; and Borejdo and Burghardt, 1987). Myosin heads are oriented within a certain range of polar angles with azimuthal symmetry about the fiber axis, yielding a cone-shaped orientational probability distribution. The formalism required to derive this probability distribution from fluorescence measurements is considerably more complicated than what is needed for quantitating the degree of nematic liquid-crystal ordering in acrylodan-labeled F-actin solutions. Five factors contribute to the simplicity of our calculations: (*a*) the actin filament ordering is nematic; (*b*) the actin-bound acrylodan (6-acryloyl-2-(dimethylamino)-naphthalene) probe is nearly immobile during its fluorescence lifetime (Marriott et al., 1988); (*c*) the absorption and emission dipoles of acrylodan are parallel to one another in our operating range of wavelengths (Weber and Farris, 1979; Marriott et al., 1988); (*d*) these dipoles were found to be perpendicular to the filament axis (see below); and (*e*) the acrylodan label has no detectable effect on the polymerization kinetics of actin (Marriott et al., 1988).

The principal contribution of this paper is a new and simple method, based on polarization-of-fluorescence measurements, for obtaining the absolute degree of orientational organization (nematic order parameter) in solutions of F-actin labeled with acrylodan.

We also report that the isotropic-to-nematic phase transition is continuous and temperature dependent. Above a certain filament-length threshold, the degree of ordering increases monotonically with length; above a certain filament concentration threshold, it increases monotonically with concentration. We also include qualitative descriptions of some common F-actin liquid crystal textures (geometric patterns of the director), and we show that these patterns are not dependent on sustained ATP hydrolysis.

MATERIALS AND METHODS

All experiments were carried out at room temperature unless otherwise specified. G-actin was always kept at 0° or 4°C.

Buffers

G-buffer consisted of 2 mM Hepes, 0.1 mM $CaCl_2$, 0.2 mM ATP, pH adjusted to 7.5 with NaOH. F-buffer = G-buffer + 50 mM NaCl and 2 mM $MgCl_2$.

Actin and gelsolin

Actin was purified from rabbit skeletal muscle according to the procedure of Mommaerts (Mommaerts, 1952) with one extra polymerization-depolymerization cycle, and usually further purified by gel filtration (G-100 Sephadex) with one final polymerization-depolymerization cycle. F-actin was stored as a pellet at 0°C. Before each experiment a G-actin solution was prepared by homogenizing an F-actin pellet in an appropriate volume of G-buffer (depending on the desired final concentration) with 1 mM dithiothreitol (DTT), dialyzing the homogenate exhaustively against G-buffer, then clarifying the solution by centrifugation at 10^5 *g* for 30 min. The supernatant was thoroughly degassed to prevent the formation of bubbles during polymerization. Gelsolin, purified by affinity chromatography, was kindly provided by Dr. Paul Janmey (Massachusetts General Hospital) and stored at −70°C.

Samples for length vs. concentration phase diagram

Six G-actin solutions having concentrations ranging from 0.02 to 4.13 mg/ml were each split into six aliquots, for a total of 36 samples. Gelsolin was added to the aliquots to form heterotrimer nuclei consisting of one gelsolin molecule and two bound actin molecules (GA_2) (Coué and Korn, 1985). Assuming a one-to-one stoichiometry between the gelsolin concentration and the filament concentration after polymerization (Coué and Korn, 1985), the mean number of subunits per filament after polymerization would equal the actin-to-gelsolin molar ratio. With the knowledge that a filament contains 366 actin molecules per μm, the gelsolin concentrations were chosen to yield final mean filament lengths of 1, 5, 10, 20, 30, and 50 μm at each of the six concentrations. A calculation based on an approximate model of polymerization kinetics reveals that the filament length distribution remains narrow until polymerization is complete (within the first 15 min). Subsequently, while the mean length remains stable, the standard deviation continues to increase for many days. After 1 wk, the standard deviation would be ~50% of the mean (see Appendix 1).

3.2 μl of each sample were taken up into a 4 μl capillary tube (internal diameter, 0.31 mm); then 0.8 μl of concentrated salt solution (5 M NaCl, 0.2 M $MgCl_2$) was taken up into each tube adjacent to the actin solution. Care was taken to prevent the incorporation of an air bubble between the salt and protein solutions. The ends of the tubes were sealed with molten parafilm, and the actin was polymerized by allowing the salt to diffuse into the actin solutions at 4°C for ~20 h.

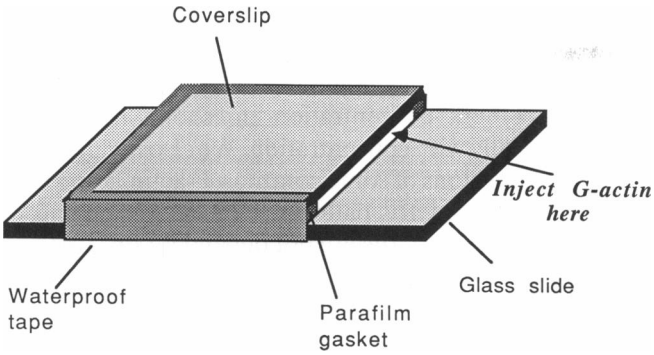

SCHEME 1

Samples for temperature-dependence measurements

Different amounts of gelsolin were added to three 0.8 ml aliquots of 2.0 mg/ml G-actin to achieve actin-to-gelsolin ratios that would yield filaments having mean lengths of 1, 10, and 20 μm. Polymerization was initiated after 15 min raising the salt concentration to 50 mM NaCl, 2 mM $MgCl_2$; then the samples were mixed by multiple suctions with a pasteur pipette, and immediately transferred to 1-ml quartz cuvettes (10×2 mm cross-section), and left undisturbed until the end of the experiment. The polymerization reaction was given at least 1 h.

Measurements of temperature dependence of intensity of light transmitted through crossed polarizers

The three aforementioned cuvettes were placed together between crossed Glan-Thompson polarizers in the thermostated sample holder of a SPEX Fluorolog 2/2/2 spectrofluorometer (SPEX Industries, Edison, NJ), which was operated in the transmission mode at a wavelength of 400 nm. The pathlength of light through the samples was 1 cm. After equilibration at 46°C, the intensity of the transmitted light was monitored as the temperature was decreased continuously at a rate of 10°/h.

Preparation of an undistorted F-actin liquid crystal

The following method relies on slow polymerization by diffusion of salt into the G-actin solution; it bypasses the mixing step which usually causes irreversible distortions in the incipient liquid crystal by orienting oligomers in a turbulent flow.

A U-shaped, five-layer thick parafilm gasket was sandwiched between a clean glass slide and a coverslip, then melted in place with very gentle heating from a desk lamp. (It was important not to overheat it.) Then the three sides of the gasket were sealed with waterproof tape. One side was left open for introducing ~300 μl of degassed G-actin solution by capillary action (scheme 1).

Once the solution was in place, the slide was gently immersed in ~300 ml of degassed F-buffer, where it remained horizontal and free of vibrations for 7 d. Then it was gently retrieved from the bath and held vertically (open end up); the outside was dried with tissue paper, without disturbing the meniscus, and the open end was finally sealed with waterproof tape to prevent dehydration. The sample was stored vertically in a damp environment, at room temperature, until it was used for fluorescence measurements.

Determination of linear birefringence

A Zeiss Axiovert fluorescence microscope equipped with a rotating stage and a photomultiplier tube was used as a polarizing microscope. The incident light from a tungsten lamp was first passed through a narrow bandpass interference filter (λ = 599.7 nm, bandwidth 8.8 nm), then through a Glan-Thompson polarizer. The condenser tube, equipped with a pair of irises, was used without a lens to select collimated incident light, and the objective lens was replaced by a hollow 4 cm long cylinder with a wide pinhole at each end to select collimated transmitted light. The depolarizing effects of high numerical aperture lenses were thereby avoided. The transmitted light was finally passed through a polaroid-type film analyzer.

The intensity of the light, I_{trans}, transmitted through a birefringent medium, placed between crossed polarizers, whose optic axis is perpendicular to the direction of illumination is:

$$I_{trans} = I_{inc} \frac{\sin^2(2\varphi)}{2}\left[1 - \cos\left(\frac{2\pi z \Delta n}{\lambda}\right)\right] + B, \qquad (1)$$

where I_{inc} is the intensity of the incident light, φ is the angle between its plane of polarization and the optic axis of the sample (parallel to the director), z is the pathlength, Δn is the birefringence, λ is the wavelength, and B is the background signal. I_{inc} was measured with the planes of polarization of the polarizer and analyzer parallel, while no sample was on the stage. B was measured with the polarizer and analyzer crossed (90°), while the optic axis of the sample was oriented parallel to the incident polarization. The thickness of the sample was measured with a micrometer. The birefringence was calculated by solving Eq. 1 for Δn.

Labeling with acrylodan

50 ml of 0.5 mg/ml G-actin solution were dialyzed exhaustively against G-buffer containing no reducing agent. Insoluble material was removed by sedimentation, then the actin was polymerized by raising the salt concentration to 50 mM NaCl, 2 mM $MgCl_2$. Acrylodan powder was dissolved in 150 μl of dimethylformamide (DMF), and then added in 25 μl portions to the F-actin solution, with gentle mixing between each addition. The final acrylodan-to-actin molar ratio was 3:1. The reaction was allowed to proceed with gentle mixing, for ~15 h, at room temperature, in the dark. The actin filaments, and some precipitate, were sedimented ($10^5 g$, 30 min), and then the pellets were homogenized in a total of 10 ml of G-buffer containing 1 mM DTT. The homogenate was then dialyzed against the same buffer, for 24 h at 0°C, to remove the remaining salt and allow the actin to depolymerize. Any remaining insoluble material was removed by sedimentation, followed by filtration of the supernatant (1.2 μm pores). The actin in the supernatant was further purified by gel filtration (G-100 Sephadex) in order to remove any unbound acrylodan. The final degree of labeling of the purified actin was ~40%, and ~25% of the original protein was lost. The partially labelled acrylodan-actin (AA) was polymerized, sedimented, and stored in pellets at 0°C in the dark.

Determination of the angle between the acrylodan transition dipole and the filament axis

As mentioned above, the emission dipole of acrylodan has been shown to lie parallel to the absorption dipole for excitation wavelengths in the range of 320–450 nm (Weber and Farris, 1979, Marriott et al., 1988); and acrylodan has been shown to remain nearly immobile during its fluorescence lifetime (Marriott et al., 1988).

Since the actin filament is helical, the static orientational distribution of the acrylodan dipoles must be symmetrical about the filament axis. In order to derive the nematic order parameter (degree of filament alignment) from polarized fluorescence measurements, the polar an-

gle, μ, between the transition dipoles and the filament axis must first be determined. This angle was obtained approximately by comparing measurements of polarized fluorescence from a solution of labeled actin filaments that had been artificially aligned in a steep flow velocity gradient, with the expected polarized fluorescence calculated for a series of different values of μ and a series of different degrees of alignment.

A 1-ml sample of 3.59 mg/ml F-AA was loaded into a syringe with no air pocket. The entire volume was flowed at high speed through a 70-cm long segment of Tygon tubing (ID = one-thirty second of an inch) connected to a thin rectangular capillary tube ($50 \times 3 \times 0.2$ mm). The flow velocity gradient transverse to the long axis of the capillary tube caused the filaments to become aligned with this axis. The solution was allowed to flow out of the opposite end of the capillary tube until the syringe was empty, while the Tygon tubing and the capillary tube were still full. The capillary tube was disconnected and sealed at both ends with molten parafilm.

Fluorescence measurement were made with the Axiovert microscope in the epifluorescence mode (exciting and emitted light propagating along the same axis), with excitation wavelengths below 400 nm and emission above 470 nm, using a 40 × objective lens. Polarizations are defined in terms of the following rectangular laboratory coordinates. Light propagated along the X axis; the intersection between the (sagital) plane of symmetry of the microscope and the plane of the stage defined the Z axis; and the Y axis was perpendicular to X and Z. The polarizations of the polarizer and analyzer could be made parallel to either Y or Z, and will be referred to in that order (e.g., "$Z\,Y$ configuration" means polarizer parallel to Z, analyzer parallel to Y). The fluorescence intensities I_{ZZ} and I_{ZY} were measured as a function of the orientation of the capillary in the Y-Z plane.

The orientation of a dipole can be described relative to the laboratory frame in terms of a polar angle θ between the Z axis and the dipole, and an azimuthal angle φ between the X axis and the projection of the dipole onto the X-Y plane (see scheme A2.1). The probability of excitation of the dipole by incident light polarized parallel to Z is proportional to $\cos^2\theta$. The probability of emission with polarization parallel to Z is also proportional to $\cos^2\theta$, whereas the probability of emission with polarization along Y is proportional to $\sin^2\theta\sin^2\varphi$. Thus, the polarized intensities of the light emitted from that single dipole should be $I_{ZZ} = g\cos^4\theta$ and $I_{ZY} = g\cos^2\theta\sin^2\theta\sin^2\varphi$, where g is a constant.

For calculating the expected fluorescence, the orientational distribution of the filaments about the director (which is parallel to the long axis of the capillary) was presumed to be Gaussian in the plane of the flat capillary.

The computer program summed the contributions to I_{ZZ} and I_{ZY} from a statistical number of dipoles in the aforementioned distribution, and then repeated the procedure as it rotated the director in the Y-Z plane in 5° increments to generate a polar plot. Polar plots for I_{ZZ}, I_{ZY}, and the ratio I_{ZZ}/I_{ZY} were generated for values of μ (the angle between the dipole and the filament) and of σ (the standard deviation of the Gaussian) ranging from 0 to 90° in increments of 10°. Thus, 300 plots were generated for comparison with the experimental plots.

Investigation of the potential role of ATP hydrolysis in liquid crystal texturing

Two 3.4 mg/ml G-actin samples, one containing 0.2 mM ATP and the other 0.2 mM ADP were allowed to dialyze exhaustively against their respective buffers, then cleared by centrifugation and degassed. 1.3 ml of these solutions was introduced vertically into separate glass containers consisting of two clean microscope slides separated by a 1 mm thick, U-shaped parafilm gasket that had been gently melted in place and sealed along three edges with waterproof tape. An equal volume of degassed F-buffer, containing 0.2 mM of either ATP or ADP, and 100 mM NaCl and 4 mM $MgCl_2$, was then gently injected at the bottom of each container with a long needle. The open end of each container was then given an airtight seal. The boundary between the actin solution in the upper layer, and the F-buffer in the lower layer, remained very sharp. There was no mixing, except for a small disturbance in the ADP-containing sample, caused by two small air bubbles rising from the bottom through the two layers. After slowly equilibrating between the two layers, the final uniform salt concentration would eventually reach 50 mM NaCl and 2 mM $MgCl_2$.

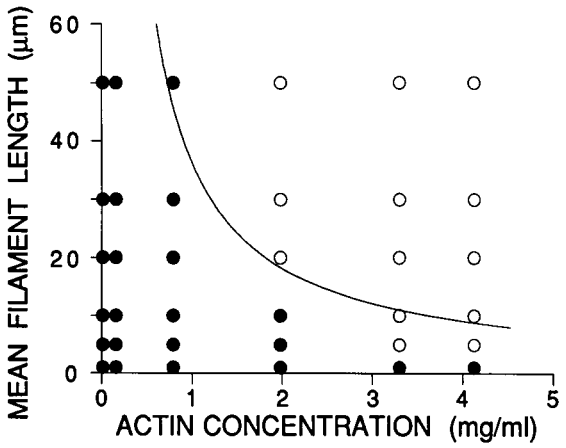

FIGURE 1 Phase diagram showing the concentrations and mean filament lengths at which F-actin solutions were either completely isotropic (*black symbols*) or had varying degrees of anisotropy (*open symbols*). The curve is the predicted phase boundary $v = (8/x)(1 - 2/x)$ derived by Flory (Flory, 1956a) for the emergence of an anisotropic phase in monodisperse solutions of noninteracting rigid cylinders.

RESULTS

Length versus concentration phase diagram

Each of the 36 capillary tubes containing actin at concentrations ranging from 0.02 to 4.13 mg/ml and mean filament lengths ranging from 1 to 50 μm was observed with 40 × magnification under the polarizing microscope. The actin solutions were scored qualitatively as birefringent (transmitting light) or nonbirefringent. The edges of the tubes were ignored, because they always transmitted light due to depolarizing refraction effects at the curved surfaces. All of the samples, except some of the 1 μm samples, were either homogeneously birefringent or nonbirefringent. Coexisting isotropic and anisotropic domains were not observed in any of the samples. However, some of the 1 μm samples contained a few tiny, scattered, oddly shaped, and strongly birefringent crystalline objects. These objects contained a black cross whose arms were always parallel to the polarization planes of the polarizer and analyzer regardless of the orientation of the sample. This indicates a radially symmetric orientational distribution of the crystalline optic axis in these objects. The solution surrounding the little crystals was always completely nonbirefringent, however, so these samples were scored as such.

In Fig. 1, each sample is plotted according to its actin concentration and mean filament length as a white circle

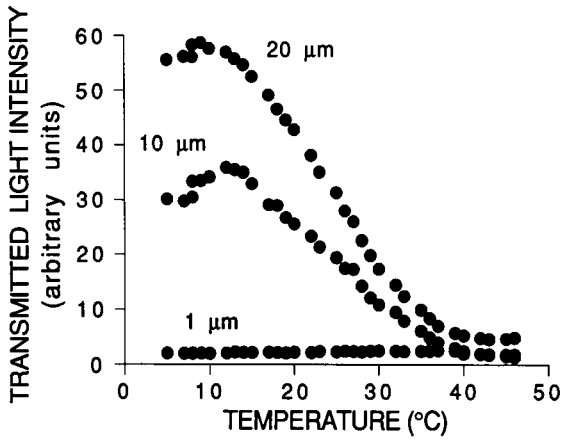

FIGURE 2 Temperature dependence of the intensity of light transmitted through 2.0 mg/ml F-actin solutions placed between crossed polarizers. Mean filament length fixed at 1, 10, and 20 μm by gelsolin-induced nucleation.

if it was birefringent, or as a black circle if it was not. The curve drawn through the plot is the phase boundary $v = (8/x)(1 - 2/x)$ predicted by Flory (Flory, 1956*a*) for a monodisperse solution of noninteracting rigid cylinders, where v is the volume fraction occupied by the cylinders, and x is their length-to-diameter ratio. Assuming that the actin filament is a cylinder with a 70 Å diameter and a length of 28 Å per subunit, this phase boundary can be rewritten as $F = (36.36/L)(1 - 0.014/L)$, where F is the F-actin concentration in mg/ml, and L is the mean filament length in μm. The experimental phase boundary lies close to this curve but at slightly shorter lengths, indicating that the actin filaments have a higher propensity to line up than do the cylinders in Flory's model.

Temperature dependence of orientational ordering

The intensity of light transmitted through solutions, placed between crossed polarizers, containing 2.0 mg/ml F-actin with mean filament lengths of 1, 10, and 20 μm, was monitored as the temperature was decreased slowly from 46° to 5°C (Fig. 2). When initially viewed between crossed polarizers with back illumination at 46°C, each sample appeared completely nonbirefringent.

The samples containing 10 and 20 μm filaments became increasingly anisotropic with decreasing temperature, whereas the sample containing 1 μm filaments remained optically isotropic at all temperatures in this range. The intensity of the light transmitted by the 20 μm filaments was about twice as great as that transmitted by the 10 μm filaments. In both cases, the intensity reached a maximum at a temperature of ~10°C, then declined slightly at lower temperatures. These measurements show that F-actin solutions become increasingly ordered with decreasing temperature, and that long filaments become more readily aligned than short ones. Another important observation is that the temperature-dependent transition from the isotropic state to the anisotropic one is gradual, i.e., there are no discontinuities in Fig. 2.

Specificity of the labeling site

Acrylodan is a thiol-reactive probe that reportedly reacts specifically with actin's single highly reactive cysteine residue (Cys 374) (Marriott et al., 1988). However, the possibility of also labeling less reactive sites must be considered. The result of a fluorescence decay experiment supported the contention that a single site was labeled. A superposition of two fluorescence lifetimes of 5.57 and 0.78 ns gave the best fit to the fluorescence decay kinetics for a solution containing acrylodan-labeled G-actin and some free unreacted acrylodan. After polymerization, the lifetimes were 5.14 and 0.79 ns, respectively. The short lifetime, that is insensitive to the polymerization state of the actin, corresponds to free acrylodan. The long lifetime must correspond to a single labeled site according to the following reasoning. If there were two (or more) labeled sites with different lifetimes our fitting would have been a forced-fit of a double exponential to a triple (or higher order) exponential experimental curve; changes in the lifetimes of the labeled sites with polymerization would have affected both of the force-fitted double-exponential lifetimes. That wasn't the case, as the short lifetime remained virtually unchanged. Therefore, we conclude that only two lifetimes contributed to the experimental fluorescence decay: one corresponding to free acrylodan, and one corresponding to acrylodan bound to a single site on actin. It must be recognized, nonetheless, that while this experiment is highly suggestive of site-specific labeling, it doesn't afford an incontrovertible proof that this is the case. There is a very small chance that probes at several different sites could all have the same initial lifetime before polymerization, and the same new lifetime after polymerization.

Angle, μ, between the acrylodan dipole and the filament axis

Polar plots of the experimental values of I_{ZZ}, I_{ZY}, and I_{ZZ}/I_{ZY} as a function of the orientation of the flat capillary (containing the 3.6 mg/ml solution of actin filaments oriented by flow) were compared with those calculated numerically for various values of μ and σ. The best fit was obtained for $\mu = 90°$ and $\sigma = 20°$. The experimental and simulated polar plots are shown side by side in Fig. 3. Since the simulated plots were generated for values of μ and σ at intervals of 10°, the uncertainty in determining the actual values of these angles was ±5°.

The 20° standard deviation could be attributed to three possible forms of disorder: (*a*) disorder of the probe orientation on the filament, (*b*) curvature of the

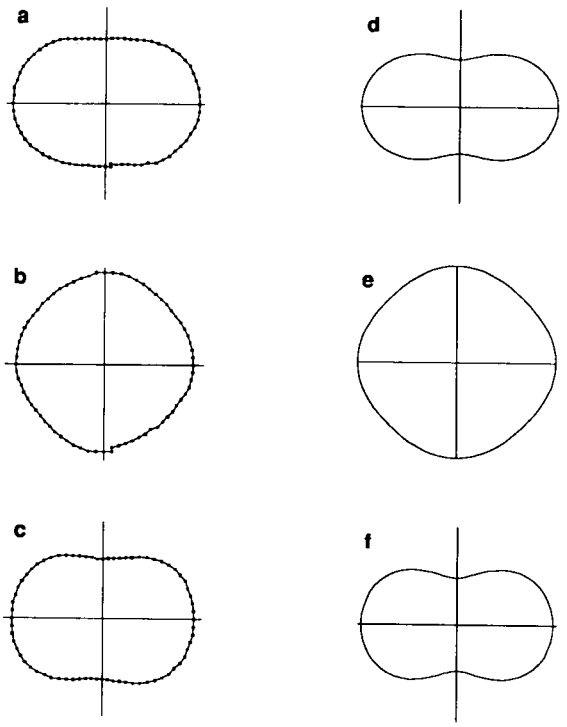

FIGURE 3 Polar plots of I_{ZZ}, I_{ZY}, and I_{ZZ}/I_{ZY} as a function of sample orientation with respect to the crossed polarizers for a 3.6 mg/ml F-acrylodan-actin sample in which the filaments were aligned by flow (*a*, *b*, *c*, respectively), and calculated from first principles assuming σ = 20°, μ = 90° (*d*, *e*, *f*, respectively). (σ is the standard deviation of the presumed Gaussian orientational distribution about the director in the plane of the flat capillary; and μ is the angle between each bound dipole and the filament axis.)

filaments, and (*c*) poor alignment of filaments with one another. The effect of probe disorder is minimal because of its rigid attachment to actin. Filament curvature is inevitable; it permits some disorder about the "average orientation" of each filament, and it also allows more rapid relaxation of flow-induced interfilament alignment after the flow has ceased. Since there was no meandering of the optic axis in the capillary, there could have been no widespread side-by-side parallel bending of adjacent filaments; therefore, most of the measured disorder must have reflected interfilament misalignment.

Determination of the nematic order parameter

The nematic order parameter, s, is a measure of the mean degree of filament alignment along the director, which is given by a polar angle θ_c between the director and a unit vector $\hat{\mathbf{c}}$ parallel to the filament. The order parameter s_c is defined as (de Gennes, 1974):

$$s = \tfrac{1}{2}\langle 3\cos^2\theta - 1\rangle, \qquad (2)$$

where the subscript c has been dropped because the filament axis is customarily used as the default molecular reference axis.

When the distribution of filament orientations is isotropic, $\langle\cos^2\theta\rangle = \frac{1}{3}$ and $s = 0$. When all the filaments are parallel to the director, $\langle\cos^2\theta\rangle = 1$ and $s = 1$. And when all the filaments lie perpendicular to the director, $\langle\cos^2\theta\rangle = 0$ and $s = -0.5$. So s always lies between -0.5 and 1. The order parameter of a nematic containing oblate particles (like disks) will usually lie between -0.5 and 0, whereas if the particles are prolate (like cylinders), s will usually lie between 0 and 1.

Two other unit vectors, $\hat{\mathbf{a}}$ and $\hat{\mathbf{b}}$, can be affixed to each filament. Together with $\hat{\mathbf{c}}$, these form a set of right-handed orthogonal molecular coordinates. If the filaments behave as cylindrically symmetric particles, it can be shown (de Gennes, 1974) that the order parameters s_a and s_b, corresponding to molecular axes $\hat{\mathbf{a}}$ and $\hat{\mathbf{b}}$, respectively, are related to s_c as follows:

$$s_a = s_b = -\tfrac{1}{2}s_c. \qquad (3)$$

Thus, because μ is ~90°, Eq. 3 can be used to relate the order parameter of the acrylodan dipoles directly to that of the filaments.

To calculate the filaments' order parameter independently of any experimental parameters (such as the transmission coefficients of dichroic mirrors and the quantum yield of acrylodan for example) nine measurements should be made with the director parallel to the Z axis: the polarized fluorescence intensity, I_{ij}, the background intensity, B_{ij}, and the incident light intensity, X_{ij}, where the indices ij denote ZZ, YY, and either YZ or ZY (one of these two is sufficient). The director was aligned with the Z axis by rotating the stage while measuring I_{ZZ} until a minimum was found. Denoting $z = (I_{ZZ} - B_{ZZ})/X_{ZZ}$, $y = (I_{YY} - B_{YY})/X_{YY}$, and $w = (I_{ZY} - B_{ZY})/X_{ZY} = (I_{YZ} - B_{YZ})/X_{YZ}$, the order parameter can be expressed as (see Appendix 2):

$$s = 1 - 3\frac{2w + z}{4w + \frac{8}{3}y + z}. \qquad (4)$$

Comparison of the calculated order parameter with the linear birefringence

As a verification that Eq. 4 yields reasonable values for s, simultaneous determination of s (from fluorescence measurements) and of Δn (from transmission measurements) were made on three 2.4 mg/ml F-actin solutions containing filaments of different average lengths as predetermined by the gelsolin concentration. The expected mean filament lengths were 2 μm, 10 μm, and "unknown" (no gelsolin). The birefringence is plotted as a function of the order parameter in Fig. 4. While containing only three points, this plot is consistent with the prediction that the birefringence should increase monotonically with the order parameter (De Jeu, 1980). The filaments in the gelsolin-free sample were more highly

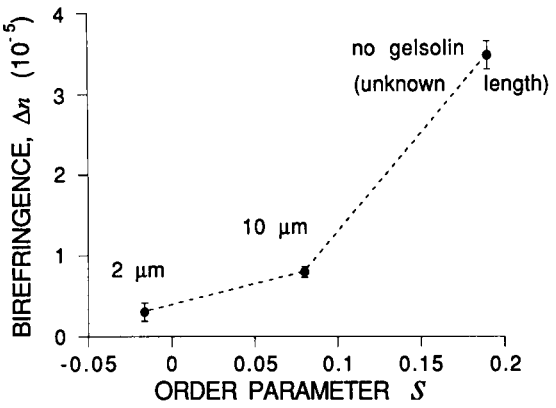

FIGURE 4 Birefringence calculated from transmission measurements plotted as a function of the order parameter calculated from fluorescence measurements for 2.4 mg/ml F-acrylodan-actin liquid crystals containing filaments of different mean length. (Assuming a good alignment of the sample's optic axis with the microscope's plane of polarization, the calculated horizontal error bars are too small to be seen in this plot.)

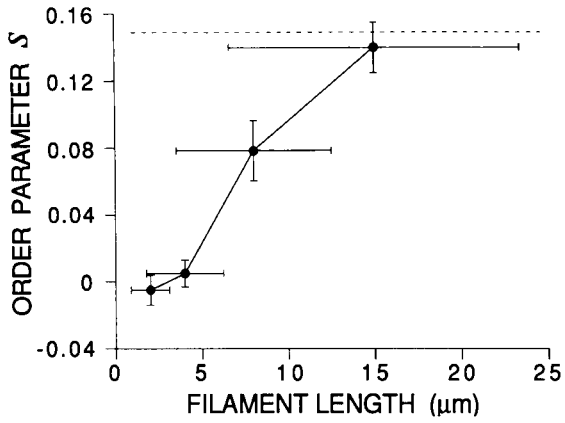

FIGURE 5 Dependence of the order parameter on mean filament length for 3.7 mg/ml F-acrylodan-actin liquid crystals. The dotted line shows the order parameter for a sample containing filaments of unknown mean length (containing no gelsolin). Each point corresponds to a mean length, and the horizontal error bars represent the standard deviation of the length distribution as calculated in Appendix 1.

ordered than in the other two samples, since they were formed through spontaneous nucleation which normally yields longer filaments.

The calculated order parameters were low (-0.015 to $+0.200$), and corresponded to values of the birefringence that would be typical of dilute F-actin solutions in which the filaments are moderately aligned in a flow velocity gradient. For the 2 μm sample, the true value of s is probably not negative, but rather zero or a very small positive number, because actin filaments are prolate particles. The very small negative value of s that was calculated for this sample reflects the inherent experimental uncertainty in aligning the optic axis of a nearly isotropic sample with the microscope's plane of polarization (the Z axis). The other two more anisotropic samples could be oriented with much higher accuracy.

Filament-length dependence of the order parameter

The order parameters of five 3.7 mg/ml F-actin liquid crystals containing filaments with average lengths of 2, 4, 8, 15, and "unknown" μm (as predetermined by the gelsolin concentration) were obtained as described above. While remaining quite low ($-0.005 < s < 0.15$), the order parameter increased monotonically with filament length (Fig. 5). The order parameter of the gelsolin-free sample containing filaments of unknown length is drawn as a dotted line in the figure. The horizontal error bars represent the calculated standard deviation of each filament length distribution (see Appendix 1). The calculated order parameter for the 2 μm filaments turned out to be a very small negative number ($s \approx -0.005$). This is again probably attributable to the experimental uncertainty in the calculated value of s for a nearly isotropic sample. The plot in Fig. 5 is consistent with the idea of a continuous phase transition from the isotropic to the ordered state, which occurs above a threshold filament length lying between 2 and 4 μm for an actin concentration of 3.7 mg/ml.

Concentration dependence of the order parameter

The order parameters of five liquid crystals containing 1.2, 1.8, 2.2, 2.6, and 3.0 mg/ml F-actin and no gelsolin were obtained as described above (Fig. 6). While the mean filament length in these solutions was unknown, it probably decreased with increasing concentration because the spontaneous nucleation rate (and therefore the filament number concentration) increases as the third or

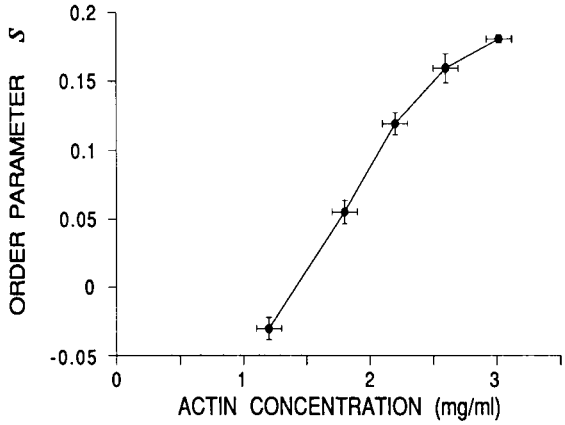

FIGURE 6 Dependence of the order parameter of F-acrylodan-actin liquid crystals on the actin concentration. The mean filament lengths are unknown.

fourth power of the initial G-actin concentration (Kasai et al., 1962).

Once again, the calculated value of s for the least ordered solution (1.2 mg/ml) turned out slightly negative. This could be attributed to the aforementioned experimental uncertainty in orienting a nearly isotropic sample. Above 1.5 mg/ml, the order parameter was a strictly positive, monotonically increasing function of the actin concentration. This means that there is a continuous phase transition from the isotropic state to an ordered state, occurring above a threshold actin concentration. The downward curvature in Fig. 6 is probably due to the expected decrease in the mean length of spontaneously nucleated filaments with increasing actin concentration.

In this experiment the order parameters again remained fairly low ($s < 0.2$). However, under physiological conditions, the actin concentration is at least ten times greater than in our most concentrated sample, and the order parameter, therefore, should be much closer to one.

Textures

Texturing refers to the smooth meandering of the orientation of the director from one place to the next within the liquid crystal. It is manifested as a convoluted pattern of black lines that changes shape as the solution is rotated between crossed polarizers with back illumination. While texturing is an interesting phenomenon that may be physiologically important, it often precludes measurement of the birefringence or of the order parameter, because these measurements require macroscopic liquid crystalline regions in which the director is invariant.

Qualitatively, the distortion due to texturing always seemed to increase with increasing polymerization rate. Liquid crystals in which the actin had been slowly polymerized by diffusion of salt always contained vast untextured areas (>1 cm^2), whereas those in which the actin had been rapidly polymerized by suddenly raising the salt concentration to 50 mM NaCl and 2 mM $MgCl_2$, almost always became completely textured. Among rapidly polymerized samples, the characteristic length scale of the director's meandering (persistence length of the director) seemed to decrease with increasing actin concentration, and therefore, with polymerization rate; hence, concentrated samples appeared more convoluted than dilute ones. There was always a delay of ~15–30 min (during polymerization) between the appearance of birefringence and the onset of texturing. Texturing always originated at one or several "nucleation sites" such as the parafilm gasket or a small air bubble, and then propagated throughout the liquid crystal at rates of up to ~1 mm/min.

While it was usually difficult to deduce the orientation of the director at every point throughout the sample, in some cases the pattern was sufficiently simple to allow a description of the texture's geometry. For example, the "zebra pattern" was quite common; it consisted of moderately aligned dark and bright stripes that would exchange place as the sample was rotated between crossed polarizers (Fig. 7). Similar patterns have previously been found in microtubule solutions (Hitt et al., 1990) and F-actin solutions (Suzuki et al., 1991). The "zebra pattern" is consistent with either a zigzaging texture (as drawn in Fig. 8) or a helicoidal texture.

F-actin liquid crystals that were prepared by adding salt to the G-actin solution, mixing, and immediately injecting the solution of polymerizing actin between a glass slide and a coverslip (separated by a thin gasket) often developed fine black striations, 10–20 μm apart, that lay perpendicular to the direction in which the solution had previously flowed, and that persisted upon rotation of the sample under the polarizing microscope. These striations indicate a twisting of the director about a screw axis with a pitch of 10–20 μm, which is reminiscent of the structure of a cholesteric liquid crystal (scheme 2). In a cholesteric liquid crystal the twisting is spontaneous, and is believed to be due to short range asymmetrical intermolecular interactions. Whereas asymmetrical interactions between actin filaments are plausible, because of the filaments' helical fine structure, the mean interfilament separation is probably too great for such interactions to have any significant effect. Furthermore, the striations were never observed in samples polymerized by salt diffusion or in samples that were sufficiently thick. Therefore, the apparent twisting was probably not due to a cholesteric liquid crystal formation, but rather to a flow instability in the solution of oligomers as it was being introduced into the thin chamber, which imparts a helicoidal texture to the nematic liquid crystal as previously described (Meyer, 1982) (scheme 3). In scheme 3 the arrow represents the orientation of the director, and the horizontal line is the direction of flow.

Some convoluted patterns in solutions of microtubules have been attributed to the putative formation of nonequilibrium energy-dissipating structures (through GTP hydrolysis) (Mandelkow et al., 1989; Robert et al., 1990; Tabony and Job, 1990) analogous to the spiral chemical waves in the Belousov-Zhabotinski reaction (Glansdorff and Prigogine, 1971). We investigated the possible role of ATP hydrolysis in the formation and persistence of patterns in F-actin liquid crystals by slowly polymerizing actin in the presence of either 0.2 mM ATP or 0.2 mM ADP, as described in Materials and Methods.

Within a few minutes of their preparation, both samples developed an untextured birefringent phase just above the upper boundary of the F-buffer layer. During the following week, the upper boundary of this birefringent region migrated upward, while the isotropic region above it shrank. The boundary between the F-buffer and the actin solution remained fixed, meaning that the rate

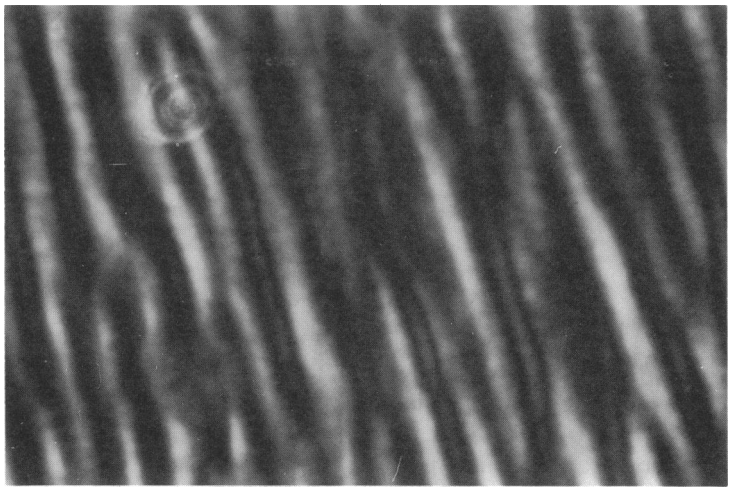

FIGURE 7 Micrograph of a zebra pattern in a 3.8 mg/ml F-actin LC. Magnification $\approx 41\times$. (The white oval is a speck of dust, on the outside of the glass, used as a reference point.)

of actin diffusion into the lower layer was extremely slow. In both samples the anisotropic, birefringent, phase contained large (>1 cm^2) homogeneous, untextured regions, flanked by textured regions, some of which were very convoluted. Qualitatively, the ATP- and ADP-containing samples were identical. The photograph shown in Fig. 9 was taken through crossed polarizers on the seventh day. The left sample contains ATP, the right one contains ADP.

DISCUSSION

Length vs. concentration phase diagram

The phase diagram contains a single phase boundary separating conditions under which F-actin solutions are uniformly isotropic from those under which they are uniformly anisotropic; it does not include the predicted region of coexistence of isotropic and anisotropic phases (Flory, 1956*b*). The experimental phase boundary lies slightly lower (shorter filaments) and to the left (lower concentrations) of the theoretically predicted boundary between an isotropic region and a biphasic region for a monodisperse solution of noninteracting rigid cylinders (Flory, 1956*b*). Therefore, the anisotropic phase forms more readily than expected. This could be due to the existence of a long range anisotropic electrostatic interaction that torques neighboring filaments into alignment with each other.

In Fig. 1, the experimental and theoretical phase boundaries seem to intersect at a filament length of ~ 30 μm. This intersection is probably due to the experimental uncertainty in attempting to predetermine filament lengths by making use of gelsolin as a nucleating agent. With decreasing gelsolin concentration, spontaneous (gelsolin-independent) nucleation becomes increasingly important. Ignoring this spontaneous nucleation leads to an underestimation of the filament concentration, and

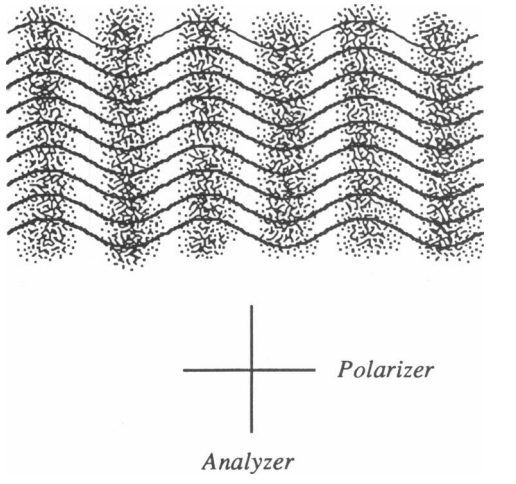

FIGURE 8 Representation of the zigzaging of the director (*solid lines*), giving rise to a series of alternating bright and dark stripes (*zebra pattern*) when the sample is viewed under the polarizing microscope.

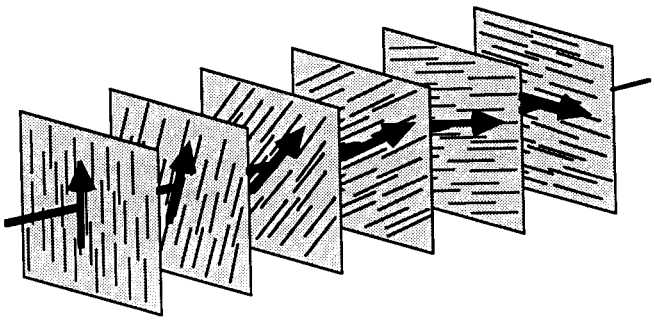

SCHEME 2

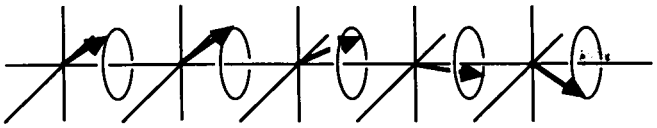

SCHEME 3

therefore, to an overestimation of the final mean filament length. Thus, the estimated mean length of short filaments is fairly accurate, whereas the estimated mean length of long filaments is probably somewhat exaggerated because of spontaneous nucleation.

Temperature dependence of orientational ordering

Dilute F-actin solutions ($\approx$2 mg/ml) containing medium filaments (10 and 20 μm) were rendered increasingly anisotropic by decreasing the temperature. This means that, under these conditions, the emergence of anisotropy was enthalpically driven while entropically unfavorable. The enthalpic contribution to the standard free energy of the solution could arise from the putative anisotropic interfilament interaction. Ordering was more readily induced by cooling solutions containing long filaments than short ones. This is consistent with excluded-volume theories (Flory, 1956*b*; Ishihara, 1951; Onsager, 1949) and with our experimental phase diagram according to which, in dilute solutions, it is entropically more unfavorable for short filaments to align than for long ones. Alignment is entropically favorable only if the filaments are sufficiently long, or if the solution is sufficiently concentrated.

In the samples containing 10 and 20 μm filaments, the anisotropy of the domain under observation increased gradually from zero with decreasing temperature, meaning that the phase transition was continuous. By contrast, a separation of coexisting isotropic and anisotropic phases would require a discontinuous phase transition.

The lack of a phase separation under any of the conditions that we used might be attributable to the slow kinetics of the filaments' translational diffusion when they are highly congested and entangled. According to Flory et al. (Abe and Flory, 1978; Flory and Abe, 1978; Flory and Frost, 1978; Frost and Flory, 1978), the phase separation occurring in a polydisperse solution of cylinders should involve the concomitant spontaneous transfer of short filaments into dilute isotropic domains, and of the long ones into more concentrated anisotropic domains. In the case of actin, this diffusion-dependent sorting process could be so slow as to render the expected phase separation experimentally unaccessible. (Even F-actin solutions that had been allowed to "age" at 4°C for up to 4 months showed no sign of phase separation.)

Length and concentration dependence of the order parameter

The development of a nonperturbating method for quantitating the nematic order parameter constitutes, in our view, a significant advance because it opens the door to the quantitative study of the effects of various actin-binding proteins on F-actin liquid crystals.

We found that, above a certain length threshold, the order parameter increases continuously with filament length; and above a certain concentration threshold, it increases continuously with concentration. Below these thresholds the solutions are isotropic. These observations were consistent with the aforementioned lack of coexistence of isotropic and anisotropic phases, which would require a discontinuous phase transition. Since the order parameter increases rapidly with concentration, one should expect a high degree of spontaneous ordering at physiological concentrations (>30 mg/ml in the cytoplasm of some locomoting cells). The existence of cytoplasmic domains containing a high concentration of isotropically oriented filaments must, therefore, require accessory proteins that cross-link the filaments in an orthogonal lattice (Stossel, 1990). In the cytoplasm, the ordered phase can be spontaneous whereas the isotropic one must be induced; not the other way around!

Textures

Texturing of the F-actin liquid crystal might be of considerable physiological importance. A liquid crystal in

FIGURE 9 Photograph, taken between crossed polarizers, of 3.4 mg/ml F-actin liquid crystals polymerized for 7 d in the presence of 0.2 mM ATP (*left*) or ADP (*right*), by diffusion of salt from the lower, isotropic, layer of F-buffer (which contained 100 mM NaCl and 4 mM $MgCl_2$). Actual size.

which the orientation of the director is always uniform and non modulatable would be of little use in the control of cell shape and motility. In contrast, a sensitive actin liquid crystal capable of rapidly adopting a variety of textures could account for the cooperative reorganization of a statistical number of cytoplasmic microfilaments in response to a localized disturbance (from the membrane for example).

How are textures formed and what determines their geometry? In most cases, we don't know. The twisted texture that we observed was induced by flow, and is therefore probably not physiologically relevant. In contrast, the zigzaging texture giving rise to the zebra pattern was spontaneous, and its formation can be tentatively explained as follows. At a salt concentration of 50 mM NaCl and 2 mM $MgCl_2$, polymerization is very rapid. Having reached a state of moderate alignment and entanglement, the filaments could still be elongating very rapidly, while the rate of alignment would become gradually slower because of steric constraints; thus, the increase in filament alignment would lag behind the polymerization reaction. Each filament would attempt to elongate further in spite of the lack of available space in the poorly ordered solution (nonaligned adjacent filaments would attempt to intersect). With further polymerization, a stress could develop in the liquid crystal, analogous to the stress in a metal plate under thermal expansion when its edges are fixed in place.

The stress could be relieved by a warping, or a corrugation of the director, beginning at the boundary. In some cases a slight disturbance may be required to trigger the corrugation. If polymerization is slow, the increase in the degree of alignment has a better chance of keeping up with the elongation of the filaments, and corrugation is less likely. If, on the other hand, polymerization is fast, but there is no perturbation, the stress may slowly dissipate as the filaments align, and corrugation may again be averted. Thus, certain cytoskeletal architectures could be achieved, at least in part, through the physiological control of the rate of actin polymerization. Numerous other textures, more complicated than the zigzaging one, have been observed, and will be the subject of further investigations.

SUMMARY

(*a*) Sufficiently concentrated F-actin solutions containing sufficiently long filaments spontaneously form a nematic liquid crystal because of excluded volume (entropic) effects and, possibly, orientation dependent interfilament interactions. (*b*) The phase transition is continuous, which explains why we never observed coexisting isotropic and anisotropic domains. The predicted phase separation, while possibly being energetically favorable, might be kinetically prohibited. (*c*) The order parameter of untextured, acrylodan-labeled F-actin liquid crystals was derived from measurements of polarized fluorescence, and was found to increase continuously with filament length and with actin concentration above a certain threshold. (*d*) F-actin liquid crystals can become textured through what appears to be an ATP-independent nucleated process whose likelihood increases with polymerization rate.

APPENDIX 1

Estimate of the length distribution of filaments nucleated with gelsolin

In some of our F-actin solutions the mean number of subunits per filament was predetermined by the actin-to-gelsolin ratio. Each gelsolin molecule nucleates one filament and then remains tightly bound to the last two actin subunits at its barbed end. Whereas the mean length remains constant after polymerization is complete, the width of the distribution continues to increase for many days. In this appendix we calculate the expected time course of the length distribution for a representative experimental sample.

P_N is the probability that a filament will contain N subunits; k_f is the "forward" (association) rate constant, and k_b is the "backward" (dissociation) rate constant for the binding of a subunit to the pointed end of a filament. These rate constants have been shown to be 0.1 $\mu M^{-1}s^{-1}$ and 0.4 s^{-1}, respectively, in the presence of ATP under the ionic conditions used in our experiments (see Korn et al., 1987, for review on polymerization rate constants).

A simple (first approximation) gelsolin-nucleated polymerization model can be based on the following premises: (*a*) Polymerization begins at time $t = 0$ with a sudden rise in salt concentration. (*b*) There is no spontaneous nucleation. (*c*) Filaments contain at least two actin subunits. (*d*) The rate constants are independent of ATP hydrolysis at the free end. (*e*) The rate constants are independent of filament length. (*f*) There is no severing or reannealing of filaments.

The differential equations describing this model are:

Monomers:
$$\frac{dP_1}{dt} = \sum_{N=3}^{\infty} k_b P_N - \sum_{N=2}^{\infty} k_f P_1 P_N \qquad \text{(A1.1a)}$$

Dimers:
$$\frac{dP_2}{dt} = k_b P_3 - k_f P_1 P_2 \qquad \text{(A1.1b)}$$

Trimers, etc.:
$$\frac{dP_N}{dt} = k_f P_1 (P_{N-1} - P_N) - k_b (P_N - P_{N+1}). \qquad \text{(A1.1c)}$$

These equations were solved numerically for a hypothetical 71.4 μM (=3.0 mg/ml) actin sample containing 0.0614 μM gelsolin. After polymerization the mean filament length would be 3 μm, and a critical concentration of 4 μM of actin would remain unpolymerized. Eight "snapshots" of the filament length distribution at 10, 20, 30 s, 1, 2, 4, 15 min, and 1 h after the onset of polymerization are shown in Fig. A1.1 *a*. After 15 min, polymerization is nearly complete (Fig. A1.2), and the mean length has reached its final value at 3 μm while the distribution is still very narrow (shown full scale in Fig. A1.1b). Once the monomer concentration has reached a stable value, the broadening of the initially narrow distribution centered at N_0 can be derived analytically as shown by Hill (Hill, 1987):

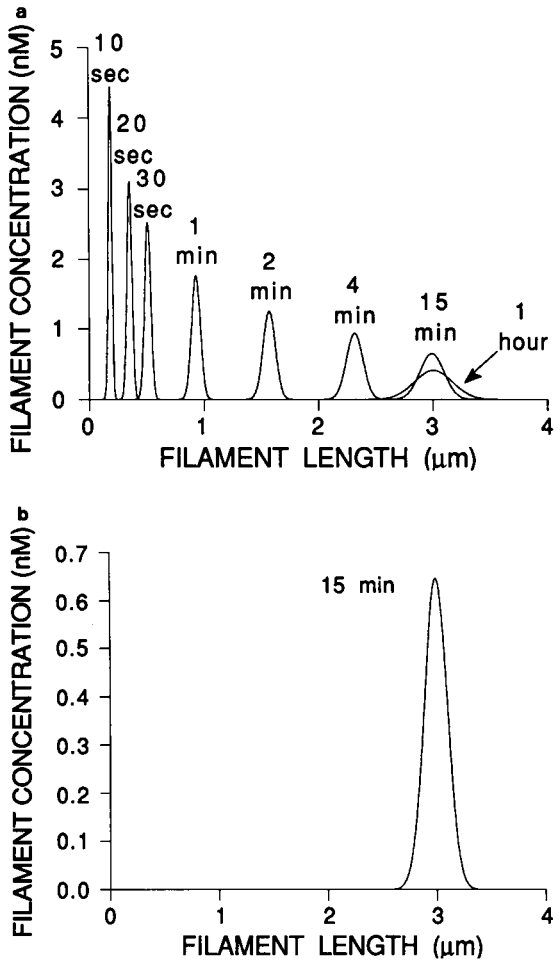

FIGURE A1.1 Calculated time course of the filament length distribution for a hypothetical 3.0 mg/ml F-actin solution in which the filaments were nucleated with 0.0614 μM gelsolin, and subsequently elongated at their pointed ends to yield a final mean length of 3 μm (*a*). After 15 min, the mean length has stabilized, and the distribution is still quite narrow (shown full scale in *b*).

$$P_N(t) = \frac{1}{2}(\pi k_b t)^{-1/2} \times \left\{\exp\left[-\frac{(N-N_0)^2}{4k_b t}\right] + \exp\left[-\frac{(N+N_0)^2}{4k_b t}\right]\right\}. \quad \text{(A1.2)}$$

The length distribution after 1 wk is shown in Fig. A1.3. The standard deviation is 57% of the mean. This relative width was used to calculate the horizontal error bars in Fig. 5.

APPENDIX 2

Calculation of the nematic order parameter from fluorescence measurements

The acrylodan dipole orientation relative to the laboratory frame is shown in scheme A2.1. The director coincides with the Z axis; light propagates along the X axis; and selected polarizations are parallel to the Z or Y axes.

The probabilities of excitation with incident light polarized parallel to Z and Y are, respectively, $P_{ex,Z} = \cos^2\theta$ and $P_{ex,Y} = \sin^2\theta \sin^2\varphi$. The

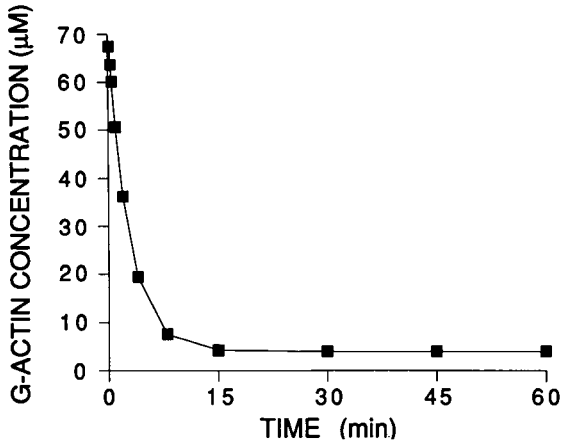

FIGURE A1.2 Calculated time course of the G-actin concentration during polymerization for the F-actin sample whose time-dependent filament length distribution is shown in Fig. A1.1. Polymerization is nearly complete after 15 min.

probability of emission with polarization parallel to Z and Y are, respectively, $P_{em,Z} = \cos^2\theta$ and $P_{em,Y} = \sin^2\theta \sin^2\varphi$.

Consider an ensemble of dipoles with a cylindrically symmetrical orientational distribution about Z, and denote the measured intensity as I_{ij}, the incident intensity as being proportional to X_{ij}, the background intensity as B_{ij}, an unknown constant as k, and brackets as meaning an average over all dipoles. The following equations give the measured intensities:

$$I_{ZZ} = kX_{ZZ}\langle\cos^4\theta\rangle + B_{ZZ} \quad \text{(A2.1a)}$$

$$I_{ZY} = kX_{ZY}\langle\sin^2\theta\cos^2\theta\sin^2\varphi\rangle + B_{ZY} = \tfrac{1}{2}kX_{ZY}\langle\sin^2\theta\cos^2\theta\rangle + B_{ZY} \quad \text{(A2.1b)}$$

$$I_{YZ} = kX_{YZ}\langle\sin^2\theta\cos^2\theta\sin^2\varphi\rangle + B_{YZ} = \tfrac{1}{2}kX_{YZ}\langle\sin^2\theta\cos^2\theta\rangle + B_{YZ} \quad \text{(A2.1c)}$$

$$I_{YY} = kX_{YY}\langle\sin^4\theta\sin^4\varphi\rangle + B_{YY} = \tfrac{3}{8}kX_{YY}\langle\sin^4\theta\rangle. \quad \text{(A2.1d)}$$

In Eq. A2.1 the terms in φ could be uncoupled from the terms in θ because of cylindrical symmetry about Z. Now we need to get rid of k

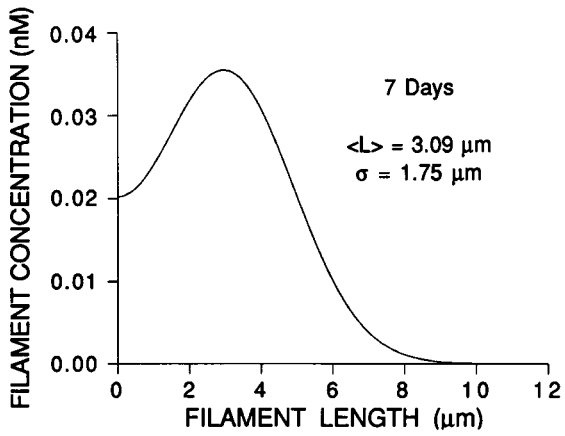

FIGURE A1.3 Calculated length distribution for the same hypothetical sample as in Fig. A1.1 after 7 d. The mean length ($\langle L\rangle$) is 3.09 μm and the standard deviation (σ) is 1.75 μm.

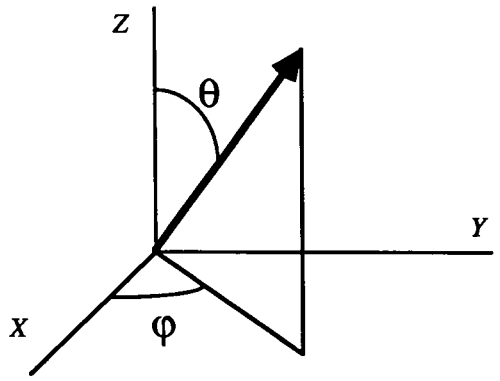

SCHEME A2.1

and express $\langle \cos^2 \theta \rangle$ in terms of the observables I_{ij}, B_{ij}, and X_{ij}. Denote: $z = (I_{ZZ} - B_{ZZ})/X_{ZZ}$, $y = (I_{YY} - B_{YY})/X_{YY}$, and $w = (I_{ZY} - B_{ZY})/X_{ZY} = (I_{YZ} - B_{YZ})X_{YZ}$, and rewrite Eq. A2.1 as:

$$\frac{z}{k} = \langle \cos^4 \theta \rangle \tag{A2.2a}$$

$$\frac{y}{k} = \frac{3}{8}\langle \sin^4 \theta \rangle = \frac{3}{8} - \frac{3}{4}\langle \cos^2 \theta \rangle + \frac{3}{8}\langle \cos^4 \theta \rangle \tag{A2.2b}$$

$$\frac{w}{k} = \frac{1}{2}\langle \sin^2 \theta \cos^2 \theta \rangle = \frac{1}{2}\langle \cos^2 \theta \rangle - \frac{1}{2}\langle \cos^4 \theta \rangle. \tag{A2.2c}$$

Now, by denoting $\langle \cos^4 \theta \rangle = u$ and $\langle \cos^2 \theta \rangle = v$, we can eliminate $k = z/u$ and rewrite Eq. A2.2 as a system of two equations in two unknowns, u and v:

$$\frac{y}{z}u = \frac{3}{8} - \frac{3}{4}v + \frac{3}{8}u \tag{A2.3a}$$

$$\frac{w}{z}u = \frac{1}{2}v - \frac{1}{2}u. \tag{A2.3b}$$

Solving for v we get:

$$v = \langle \cos^2 \theta \rangle = \frac{2w + z}{4w + \frac{3}{8}y + z}. \tag{A2.4}$$

Let $\hat{\mathbf{a}}$, $\hat{\mathbf{b}}$, and $\hat{\mathbf{c}}$ be the filament's orthogonal molecular coordinates, with $\hat{\mathbf{c}}$ parallel to the filament's long axis. Then the acrylodan dipoles, which lie at 90° to the filament axis, can be assigned to either $\hat{\mathbf{a}}$ or $\hat{\mathbf{b}}$, arbitrarily, because of cylindrical symmetry. Choose $\hat{\mathbf{a}}$ for example. Then the order parameter s_a describing the ordering of the dipoles about the liquid crystal's director can be written as:

$$s_a = {}^1/_2[3\langle \cos^2 \theta_a \rangle - 1], \tag{A2.5}$$

where the subscript a was appended to θ as a reminder that this is the angle between the dipole and the director. Finally, we can make use of the relation $s_a = s_b = -s_c/2$, to calculate the order parameter of the filaments, s_c: $s = s_c = -2s_a = 1 - 3\langle \cos^2 \theta_a \rangle$

$$s = 1 - 3\frac{2w + z}{4w + \frac{8}{3}y + z}. \tag{A2.6}$$

Eq. A2.6 yields the order parameter for the ordering of the filaments in the liquid crystal. It contains no reference to experimental and instrumental parameters such as the probe concentration or the transmission coefficients of optical filters. These parameters were all contained in the unknown constant k, which was eliminated. This derivation does assume, however, that the light is collimated along the X axis rather than being convergent. Therefore, experiments should be carried out without an objective lens.

We are very grateful to Ms. Betty Gowell for her expert technical assistance, to Dr. Sam Lehrer for invaluable advice, and to Dr. Zenon Grabarek for his critical review of the manuscript.

Supported by grants from the National Institutes of Health (HL20464) and Muscular Dystrophy Association.

Received for publication 9 January 1992 and in final form 15 May 1992.

REFERENCES

Abe, A., and P. J. Flory. 1978. Statistical thermodynamics of mixtures of rodlike particles. 2 Ternary systems. *Macromolecules.* 11:1122–1126.

Borejdo, J., and T. P. Burghardt. 1987. Cross-bridge order and orientation in resting and active muscle fibers studied by the linear dichroism of fluorescence. *In* Optical studies of muscle cross-bridges. Baskin and Yeh, editors. CRC Press, Boca Raton, FL. 99–121.

Bretsher, A. 1983. Microfilament organization in the cytoskeleton of the intestinal brush border. *Cell Musc. Motil.* 4:239–268.

Burghardt, T. P. 1984. Model-independent fluorescence polarization for measuring order in a biological assembly. *Biopolymers.* 23:2383–2406.

Burghardt, T. P. 1985. Time-resolved fluorescence polarization from ordered biological assemblies. *Biophys. J.* 48:623–631.

Burghardt, T. P., and K. Ajtai. 1988. Fluorescence polarization from oriented systems. *In* Fluorescence Spectroscopy, Vol. 2. J. R. Lakowicz, editor. Plenum Press, New York.

Coué, M., and E. D. Korn. 1985. Interaction of plasma gelsolin with G-actin and F-actin in the presence and absence of calcium ions. *J. Biol. Chem.* 260:15033–15041.

de Gennes, P. G. 1974. The physics of liquid crystals. Oxford University Press, Clarendon. pp. 23, 32.

De Jeu, W. H. 1980. Physical properties of liquid crystalline materials. Gordon & Breach, New York. p. 42.

Drenckhahn, D., K. Engel, D. Hofer, C. Merte, L. Tilney, and M. Tilney. 1991. Three different actin filament assemblies occur in every hair cell: each contains a specific actin crosslinking protein. *J. Cell Biol.* 112:641–651.

Flory, P. J. 1956*a*. Phase equilibria in solutions of rod-like particles. *Proc. R. Soc. Lond. Ser. A.* 234:73–89.

Flory, P. J. 1956*b*. Statistical thermodynamics of semi-flexible chain molecules. *Proc. R. Soc. Lond. Ser. A.* 234:60–73.

Flory, P. J. 1978. Statistical thermodynamics of mixtures of rodlike particles. 6. Rods connected by flexible joints. *Macromolecules.* 11:1141–1144.

Flory, P. J. 1984. Molecular theory of liquid crystals. Advances in Polymer Sciences. Springer-Verlag, Berlin. 2436–2472.

Flory, P. J., and A. Abe. 1978. Statistical thermodynamics of mixtures of rodlike particles. 1. Theory for polydisperse systems. *Macromolecules.* 11:1119–1122.

Flory, P. J., and R. S. Frost. 1978. Statistical thermodynamics of mixtures of rodlike particles. 3. The most probable distribution. *Macromolecules.* 11:1126–1133.

Flory, P. J., and G. Ronca. 1979. Theory of systems of rodlike particles. II. Thermotropic systems with orientation-dependent interactions. *Mol. Cryst. Liq. Cryst.* 54:311–330.

Frost, R., and P. J. Flory. 1978. Statistical thermodynamics of mixtures of rodlike particles. 4. The Poisson distribution. *Macromolecules.* 11:1134–1138.

Glansdorff, P., and I. Prigogine. 1971. Thermodynamic theory of structure, stability and fluctuations. Wiley-Interscience, New York.

Hill, T. L. 1987. Linear aggregation theory in cell biology. Springer-Verlag, New York. 46–47.

Hitt, A. L., A. R. Cross, and R. C. J. Williams. 1990. Microtubule solutions display nematic liquid crystalline structure. *J. Biol. Chem.* 265:1639–1647.

Ishihara, A. 1951. Theory of anisotropic colloidal solutions. *J. Chem. Phys.* 19:1142–1147.

Kasai, M., S. Asakura, and F. Oosawa. 1962. The cooperative nature of the G-F transformation of actin. *Biochim. Biophys. Acta.* 57:22–31.

Kerst, A., C. Chmielewski, C. Livesay, R. Buxbaum, and S. Heidemann. 1990. Liquid crystal domains and thixotropy of filamentous actin suspensions. *Proc. Natl. Acad. Sci. USA.* 87:4241–4245.

Korn, E. D., M.-F. Carlier, and D. Pantaloni. 1987. Actin polymerization and ATP hydrolysis. *Science (Wash. DC).* 238:638–644.

Luduena, M. A., and N. K. Wessells. 1973. Cell locomotion, nerve elongation, and microfilaments. *Dev. Biol.* 30:427–440.

Mandelkow, E., E.-M. Mandelkow, H. Hotani, B. Hess, and S. Müller. 1989. Spatial patterns from oscillating microtubules. *Science (Wash. DC).* 246:1291–1293.

Marriott, G., K. Zechel, and T. M. Jovin. 1988. Spectroscopic and functional characterization of an environmentally sensitive fluorescent actin conjugate. *Biochemistry.* 27:6214–6262.

Mendelson, R., and M. G. A. Wilson. 1987. Fluorescence polarization studies of myosin and muscle cross-bridges. *In* Optical Studies of Muscle Cross-bridges. Baskin and Yeh, editors. CRC Press. Boca Raton, FL. 67–98.

Meyer, R. B. 1982. Macroscopic phenomena in nematic polymers. Polymeric Liquid Crystals. Academic Press, New York.

Mommaerts, W. 1952. The molecular transformation of actin I. Globular actin. *J. Biol. Chem.* 198:445.

Mooseker, M. S. 1983. Actin binding proteins of the brush border. *Cell.* 35:11–13.

Mooseker, M. S., and C. L. Howe. 1982. The brush border of intestinal epithelium: a model system for analysis of cell-surface architecture and motility. *Methods Cell Biol.* 25:144–175.

Newman, J., N. Mroczka, and K. L. Schick. 1988. Spontaneous formation of long-range order in actin polymer networks. *Macromolecules.* 22:1006–1008.

Onsager, L. 1949. The effects of shape on the interaction of colloidal particles. *Ann. NY Acad. Sci.* 51:627–659.

Oster, G. 1950. Two-phase formation in solutions of tobacco mosaic virus and the problem of long-range forces. *J. Gen. Physiol.* 33:445–473.

Robert, C., M. Bouchiba, R. Robert, R. L. Margolis, and D. Job. 1990. Self organization of the microtubule network. A diffusion based model. *Biol. Cell. (Paris).* 68:177–181.

Stossel, T. P. 1990. How cells crawl. *Am. Sci.* 78:408–423.

Suzuki, A., T. Maeda, and T. Ito. 1991. Formation of liquid crystalline phase of actin filament solutions and its dependence on filament length as studied by optical birefringence. *Biophys. J.* 59:25–30.

Tabony, J., and D. Job. 1990. Spatial structures in microtubular solutions requiring a sustained energy source. *Nature (Lond.).* 346:448–451.

Tilney, L. G., and M. S. Tilney. 1984. Observations of how actin filaments become organized in cells. *J. Cell Biol.* 99:76s–82s.

Weber, G., and F. Farris. 1979. *Biochemistry.* 18:3075–3078.